Available online at www.sciencedirect.com
SCIENCE DIRECT®
Journal of Solid State Chemistry 177 (2004) 3375–3382
JOURNAL OF SOLID STATE CHEMISTRY
http://elsevier.com/locate/jssc

The preparation and characterization of La doped TiO_2 nanoparticles and their photocatalytic activity

Jing Liqiang,[a,b,*] Sun Xiaojun,[b,c] Xin Baifu,[a] Wang Baiqi,[b] Cai Weimin,[b] and Fu Honggang[a,*]

[a] School of Chemistry and Material Sciences, Heilongjiang University, Harbin 150080, China
[b] Department of Environmental Sciences and Engineering, Harbin Institute of Technology, Harbin 150001, China
[c] School of Chemistry and Environmental Engineering, Harbin University of Sciences and Technology, Harbin 150080, China

Received 8 January 2004; received in revised form 21 May 2004; accepted 26 May 2004

Available online 20 July 2004

Abstract

In this paper, pure and La doped TiO_2 nanoparticles with different La content were prepared by a sol–gel process using Ti$(OC_4H_9)_4$ as raw material, and also were characterized by XRD, TG-DTA, TEM, XPS, DRS and Photoluminescence (PL) spectra. We mainly investigated the effects of calcining temperature and La content on the properties and the photocatalytic activity for degrading phenol of as-prepared TiO_2 samples, and also discussed the relationships between PL spectra and photocatalytic activity as well as the mechanisms of La doping on TiO_2 phase transformation. The results showed that La^{3+} did not enter into the crystal lattices of TiO_2 and was uniformly dispersed onto TiO_2 as the form of La_2O_3 particles with small size, which possibly made La dopant have a great inhibition on TiO_2 phase transformation; La dopant did not give rise to a new PL signal, but it could improve the intensity of PL spectra with a appropriate La content, which was possibly attributed to the increase in the content of surface oxygen vacancies and defects after doping La; La doped TiO_2 nanoparticles calcined at 600°C exhibited higher photocatalytic activity, indicating that 600°C was an appropriate calcination temperature. The order of photocatalytic activity of La doped TiO_2 samples with different La content was as following: $1>1.5>3>0.5>5>0$ mol%, which was the same as the order of their PL intensity, namely, the stronger the PL intensity, the higher the photocatalytic activity, demonstrating that there were certain relationships between PL spectra and photocatalytic activity. This could be explained by the points that PL spectra mainly resulted from surface oxygen vacancies and defects during the process of PL, while surface oxygen vacancies and defects could be favorable in capturing the photoinduced electrons during the process of photocatalytic reactions.

Keywords: TiO_2; Nanoparticle; La doping; PL; Photocatalysis; Phenol

1. Introduction

In recent years, the modification as well as preparation and characterization of TiO_2 nano-sized materials has been the focus in the semiconductor photoelectric chemistry [1,2] and photocatalysis [3–5] fields. Doping is used to a kind of modification method. Rare earth metal dopant can improve the activity of TiO_2 photocatalyst [6,7]. It is well known that the surface composition and structure of photocatalyst can greatly influence their activity. PL spectrum is an effective way to investigate the electronic structure and optic characteristics of semiconductor nano-materials, by which the information such as surface oxygen vacancies and defects as well as separation and recombination of photoinduced charge carriers can be obtained [8–11]. Therefore, it is of great significance for preparing the photocatalyst with higher activity to carry out PL spectra research on semiconductor nano-materials. Here, the pure and La doped TiO_2 nanoparticles were prepared by a sol–gel process and characterized by XRD, TG-DTA, TEM, XPS, DRS and PL spectra, and their photocatalytic

*Corresponding author. School of Chemistry and Material Sciences, Heilongjiang University, Number 74, Xuefu Road, Nangang District, Harbin City 150080, Heilongjiang Province China. Fax: +86-451-86673647.
E-mail address: jlqiang@sohu.com (J. Liqiang).

0022-4596/$ - see front matter © 2004 Elsevier Inc. All rights reserved.
doi:10.1016/j.jssc.2004.05.064

activity was also evaluated by degrading phenol. The results demonstrated that the photocatalytic activity of La doped TiO_2 samples could be rapidly evaluated by measurement of PL spectra, namely, the stronger the PL intensity, the higher the photocatalytic activity.

2. Experimental

All substances were of analytical grade and used without further purification. Secondly distilled water was used in our all experiments.

2.1. Preparation of pure and La doped TiO_2 nanoparticles

The pure TiO_2 nanoparticles were prepared by a sol–gel procedure with $Ti(OBu)_4$ as raw materials [11]. 10 mL of $Ti(OBu)_4$ was mixed with 40 mL of anhydrous ethanol in a dry atmosphere. The mixed $Ti(OBu)_4$/ethanol solution was then added dropwise into another mixture consisting of 10 mL of water and 10 mL of anhydrous ethanol as well as 2 mL of 70% HNO_3 at room temperature under roughly stirring to carry out hydrolysis. Subsequently, after continuous stirring for 3 h, the yellowish transparent sol was obtained, which was allowed to stand for 6 h at room temperature and was dried at 70°C for 36 h. Thus, TiO_2 gel precursor was obtained. Finally, TiO_2 nanoparticles were gained by the thermal treatment of TiO_2 gel precursor at different temperature for 2 h and grinding.

La doped TiO_2 nanoparticles could be synthesized using almost the same method. The appropriate amount of La_2O_3 dissolved in 70% HNO_3 was added to the mixed water/ethanol solution prior to the hydrolysis of $Ti(OBu)_4$. The remaining procedures were the same as described above.

2.2. Characterization of the samples

The pure TiO_2 samples were analyzed by XRD using a Rigaku D/MAX-rA powder diffractometer, and La doped TiO_2 samples were analyzed by XRD using a Shimadzu XRD-6000 X-ray diffractometer, both with a nickel-filtered Cu$K\alpha$ radiation source.

The thermogravimetry-differential thermal analysis (TG-DTA) of La doped TiO_2 dry gel powder was performed using a Rigaku TAS 100 thermal analyzer with temperature rate of 10°C/min, α-Al_2O_3 as the referred material.

For TEM imaging with a JEOM-1200EX transmission electron microscope (TEM), the samples was dispersed in anhydrous ethanol by an ultrasonic process and a drop of the suspension was placed onto a carbon-coated copper grid. The excess liquid was removed using a paper wick and the deposit was dried in air prior to imaging. The size and morphology of TiO_2 particles were obtained from the TEM micrograph.

The surface compositions and chemical states of the samples were examined by a VG ESCALAB MKII X-ray photoelectron spectrometer (XPS) using a monochromatic aluminum X-ray source. The pressure was maintained at 6.3×10^{-5} Pa. The binding energies were calibrated with respect to the signal for adventitious carbon (binding energy = 284.6 eV). Quantitative analysis was carried out using the sensitivity factors supplied by the XPS instrument.

The diffuse reflection spectra (DRS) of the samples were recorded with a PE Lambda20 Spectrometry. The photoluminescence (PL) spectra of the samples were recorded with a PE LS 55 spectrofluorophotometer.

2.3. Evaluation of photocatalytic activity of the samples

The photocatalytic activity of TiO_2 samples was tested using phenol solution [11]. The degradation intermediates were not determined. The experiments were carried out in a 1000 mL quartz photochemical reactor, open to air, having the shape of a vertical cylinder. The light was provided from a side of the reactor by a 500 W high pressure Hg lamp without filter, which was placed at about 20 cm from the reactor, its strongest emission light is of wavelength 365 nm. The total treated volume was 800 mL, the initial concentration of phenol was equal to 0.20 mmol/L. Phenol solution was continuously stirred with a magnetic stirrer. The solution was first stirred for 20 min after 0.4 g of TiO_2 samples was added into the reaction system, it has been shown that this period was sufficient to reach the adsorption equilibrium, then began to illuminate. The phenol concentrations at different times were measured using the colorimetric method of 4-aminoantipyrine with a model 721 spectrophotometer at the wavelength of 510 nm after centrifugation.

3. Results and discussion

3.1. Measurements of XRD, TG-DTA and TEM

XRD was usually used for identification of the crystal phase and the estimation of the ratio of the anatase to rutile as well as crystallite size of each phase present. The XRD peaks at $2\theta = 25.25$ (101) and 48.0° in the spectrum of TiO_2 are easily identified as the crystal of anatase form, whereas the XRD peaks at $2\theta = 27.42$ (110) and 54.5° are easily taken as the crystal of rutile form. The XRD intensities of the anatase (101) peak and the rutile (110) peak were also analyzed. The percentage of anatase in the samples can be estimated from the respective integrated XRD peak intensities using the following equation [12]: $X(\%) = 100/(1 + 1.265 I_R/I_A)$,

where I_A represents the intensity of the anatase peak at $2\theta = 25.25°$ and I_R is that of the rutile peak at $2\theta = 27.42°$, X is the weight percentage of anatase in the sample; The crystallite size can also be determined from the broadening of corresponding X-ray spectral peaks by Scherrer formula [12]: $L = K\lambda/(\beta\cos\theta)$, where L is the crystallite size, λ is the wavelength of the X-ray radiation (Cu$K\alpha = 0.15418$ nm), K is the usually taken as 0.89, and β is the line width at half-maximum height. This is a generally accepted method to estimate the mean crystallite size of nanoparticle; In addition, the crystal lattice distortion (CLD) could also be evaluated in the light of the following equation [13]: $\varepsilon(\mathrm{CLD}) = \Delta d/d = \beta/4tg\theta$. Fig. 1 showed the XRD patterns of pure (A) and 5 mol% La doped (B) TiO_2 nanoparticles calcined at different temperature. It could be seen that the rutile phase began to appear for pure TiO_2 samples when calcining temperature was 600°C, and the anatase phase disappeared when calcining temperature was 700°C, while a little rutile phase appeared for La doped TiO_2 samples when the calcining temperature was 700°C, and even most was still anatase phase at the calcining temperature of 800°C. These demonstrated that La dopant could greatly inhibit the phase transformation from anatase to rutile, and also enhance the beginning temperature of phase transformation obviously.

Fig. 2 showed the TG-DTA curves of 5 mol% La doped TiO_2 dry gel powder. It could be found that there were two main stages from the TG curve. One was that the rate of weight loss is about 21% at the temperature range from room temperature to 450°C, which mainly resulted from the desorption or release of some substances in the gel such as adsorbed water and ethanol and the combustion decomposition of some organic matters like butanol; the other was that the weight loss was not very obvious or not even in the temperature range from 450°C to higher temperature. According to the DTA curve, a wide decalescence peak at about 100°C could be found, corresponding to the desorption of water and ethanol in the gel, and a releasing thermal peak at about 350°C was also seen, mainly due to the combustion decomposition of the organic matters. The period from about 400°C to 650°C exhibited a obvious decalescence phenomena, possibly resulting from TiO_2 phase transformation from amorphous to anatase, while the phenomena of releasing thermal at the beginning of about 700°C was attributed to the phase transformation from anatase to rutile [11]. Thus, it could also be proved that the phase transformation of TiO_2 was effectively suppressed by doping La according to the TG-DTA curves of pure [11] and La doped TiO_2 gel powder. It should be pointed that the above TG-DTA results were corresponding to the XRD ones.

The XRD data such as crystallite size, phase composition and CLD of 5 mol% La doped TiO_2 nanoparticles calcined at different temperature were shown in Table 1. It could be seen that the anatase and rutile phase crystallite size of the as-prepared TiO_2 nanoparticle samples became larger with increasing calcination temperature, while the CLD degree decreased due to the increase in the crystallite size. These demonstrated that the calcining temperature had a great

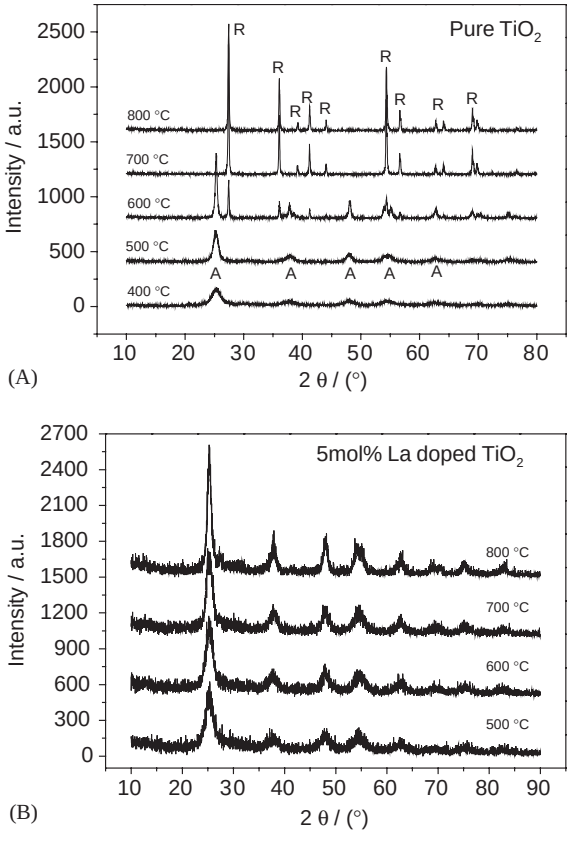

Fig. 1. XRD patterns of pure (A) and 5 mol% La doped (B) TiO_2 nanoparticles calcined at different temperature.

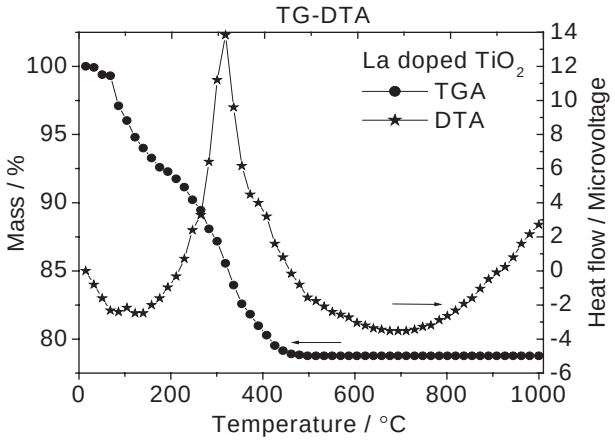

Fig. 2. TG-DTA curve of 5 mol% La doped TiO_2 dry gel powder.

Table 1
XRD data of 5 mol% La doped TiO_2 nanoparticles calcined at different temperature

La doped TiO_2 samples	Anatase crystallite size D (nm)	Rutile crystallite size D (nm)	Anatase percentage	Lattice distortion ($\Delta d/d$)	
				A101	R110
500°C	3.2		100	0.042	
600°C	4.0		100	0.036	
700°C	4.8	5.6	86.9	0.031	0.026
800°C	8.2	5.8	71.9	0.017	0.024

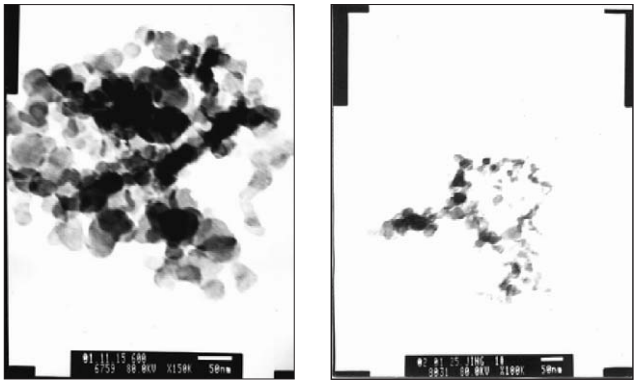

Fig. 3. TEM photographs of pure (A) and 5 mol% La doped (B) TiO_2 nanoparticles calcined at 600°C.

effect on the properties of TiO_2 samples during the preparation process.

Fig. 3 showed the TEM photographs of pure (A) and 5 mol% La doped (B) TiO_2 nanoparticles calcined at 600°C. It could be found that the pure and La doped TiO_2 nanoparticles both appeared similar sphere, with the average particle size of about 30 and 20 nm, respectively, demonstrating that La dopant could inhibit the increase of TiO_2 particle size. Moreover, both their particle sizes were larger than their crystallite ones, and it attributed to the reunion of nano-sized crystallite.

3.2. Measurement of XPS

The XPS spectra of La, O and Ti elements on the surface of 5 mol% La doped TiO_2 nanoparticles calcined at 500°C and 600°C were shown in Fig. 4. According to the principle method and handbook of the XPS instrument, the testing results demonstrated that both La elements existed mainly in the form of +3 valence in two TiO_2 samples, Ti elements were both mainly +4 valence, and both O elements had at least two kinds of chemical states, crystal lattice oxygen (1) and adsorbed oxygen (2) with increasing binding energy. Table 2 showed the XPS data of La, O and Ti elements on the surface of 5 mol% La doped TiO_2 nanoparticles calcined at 500°C and 600°C. It could be found that the amount of crystal lattice oxygen increased with increasing calcination temperature, while that of oxygen vacancies decreased. The oxygen vacancies were a very active

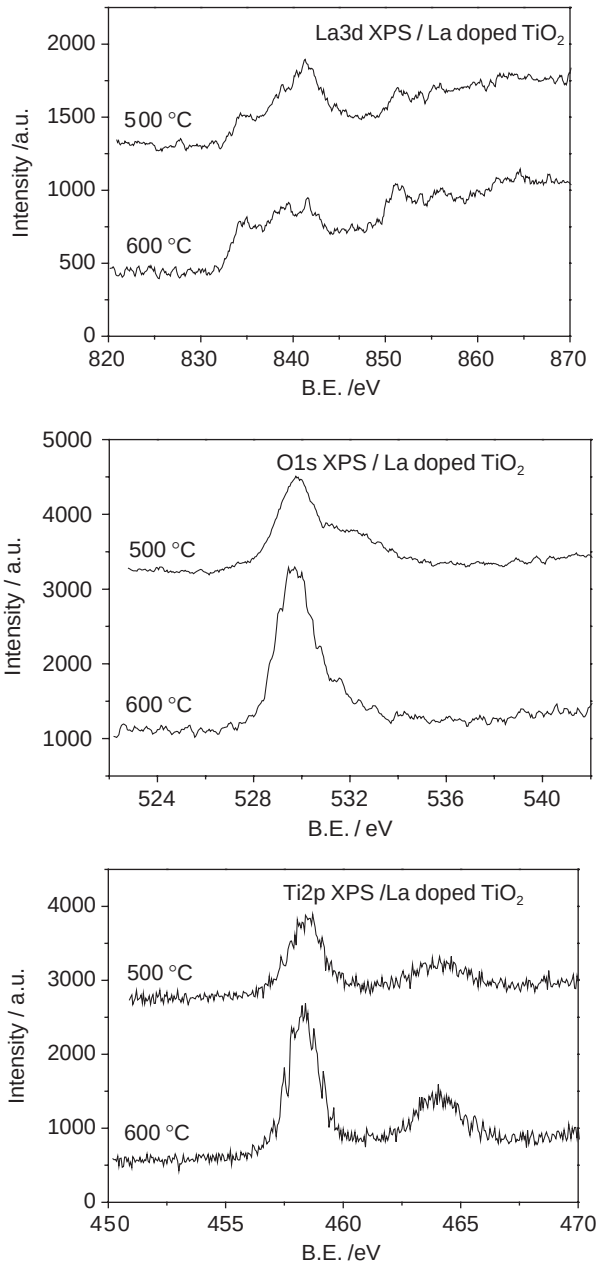

Fig. 4. XPS spectra of La, O and Ti elements on the surface of 5 mol% La doped TiO_2 nanoparticles calcined at 500°C and 600°C.

group, which easily combined with other atoms or groups to become stable. This was responsible for the existence of a certain amount of adsorbed oxygen [14].

Table 2
XPS data of different chemical states of La, O and Ti elements on the surface of 5 mol% La doped TiO_2 nanoparticles calcined at 500°C and 600°C

La doped TiO_2 (°C)	Binding energy (eV)				Atomic number ratio of O(1), Ti and La	Percentage of O(1)	Evaluated percentage of oxygen vacancies
	La3d5	O1s (1)	O1s(2)	Ti2p3			
500	834.7	529.7	532.0	458.3	100:62:2.0	62.8	27
600	834.8	529.6	531.5	458.4	100:58:2.1	75.9	19

According to Table 2, the adsorbed oxygen took up 37.2% of total oxygen on the surface of TiO_2 samples calcined at 500°C, among which at least 27% of total oxygen resulted from the oxygen vacancies. While the adsorbed oxygen took up 24.1% of total oxygen on the surface of TiO_2 samples calcined at 600°C, among which at least 19% of total oxygen resulted from the oxygen vacancies. In addition, although the ratio in mol of Ti/La elements on the surface of La doped TiO_2 nanoparticles decreased a little with increasing calcination temperature, the ratio were larger than 20:1. This demonstrated that the concentration of La in TiO_2 sample was bigger than that on the surface, and that La^{3+} easily diffused to the surface with increasing calcination temperature.

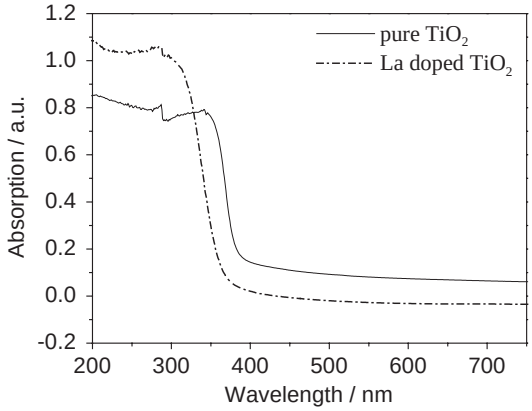

Fig. 5. DRS spectra of pure and 5 mol% La doped TiO_2 nanoparticles calcined at 600°C.

3.3. Effect mechanism of doping La on TiO_2 phase transformation

In general, the ionic radius and calcining temperature are two of the most important conditions, which can strongly influence the ability of the dopant to enter into TiO_2 crystal lattice to form stable solid solution. If the ionic radius of the dopant is much bigger or smaller than that of Ti^{4+}, the dopant substituting for TiO_2 crystal lattice ions must result into CLD. Thus, certain amount of energies can be accumulated so that the substitution process can be suppressed [15,16]. It could be seen from Fig. 1 that the XRD peaks of pure and La doped TiO_2 nanoparticles had the same positions by and large, demonstrating that La^{3+} did not enter into TiO_2 crystal lattice to substitute for Ti^{4+}. This was because the radius of La^{3+} (1.15 Å) was much bigger than that of Ti^{4+} (0.64 Å). In addition, the phase about La element could not be found in Fig. 1, possibly demonstrating that La^{3+} was dispersed uniformly onto TiO_2 nanoparticles as the form of small cluster La_2O_3. Thus, the chemical bonds of Ti–O–La three elements around the anatase crystallites could easily occur during the process of thermal treatment, which possibly inhibited producing and growing of the crystal nucleus of rutile [16].

3.4. Measurements of DRS and PL

Fig. 5 showed the DRS spectra of pure and 5 mol% La doped TiO_2 nanoparticles calcined at 600°C. Although the curve shape of the DRS spectrum of TiO_2 nanoparticles did not nearly change after La was doped, it could be found that the DRS spectrum shifted to the blue, attributed to the quantum size effect [14]. These demonstrated that La dopant did not give rise to new spectrum phenomena, and could inhibit the growth of anatase crystallite as well as the phase transformation from anatase to rutile of TiO_2, being in good agreement with the XRD results. Moreover, it could also be seen that La dopant improved the optic absorption performance of TiO_2 nanoparticles.

Fig. 6 showed the PL spectra of pure and La doped TiO_2 nanoparticles calcined at 600°C with different excited wavelength. It could be found that pure and La doped TiO_2 nanoparticles both could exhibit obvious PL signal with similar curve shape, demonstrating that La dopant did not result into new PL phenomena, while the intensity and response range of PL spectra of TiO_2 nanoparticles were influenced. In addition, TiO_2 nanoparticles could exhibit a strong and wide PL signal at the range from 400 to 500 nm with the excited wavelength of 300 nm showed in Fig. 6a, and had two obvious PL peaks at about 420 and 480 nm respectively, possibly the former mainly resulting from band edge free excitons, the latter mainly resulting from binding excitons [17,18]. There were lots of oxygen vacancies on the surface of TiO_2 nanoparticles, and the size of particle was fine so that the average distance the electrons could move freely was very short. These factors could make the oxygen

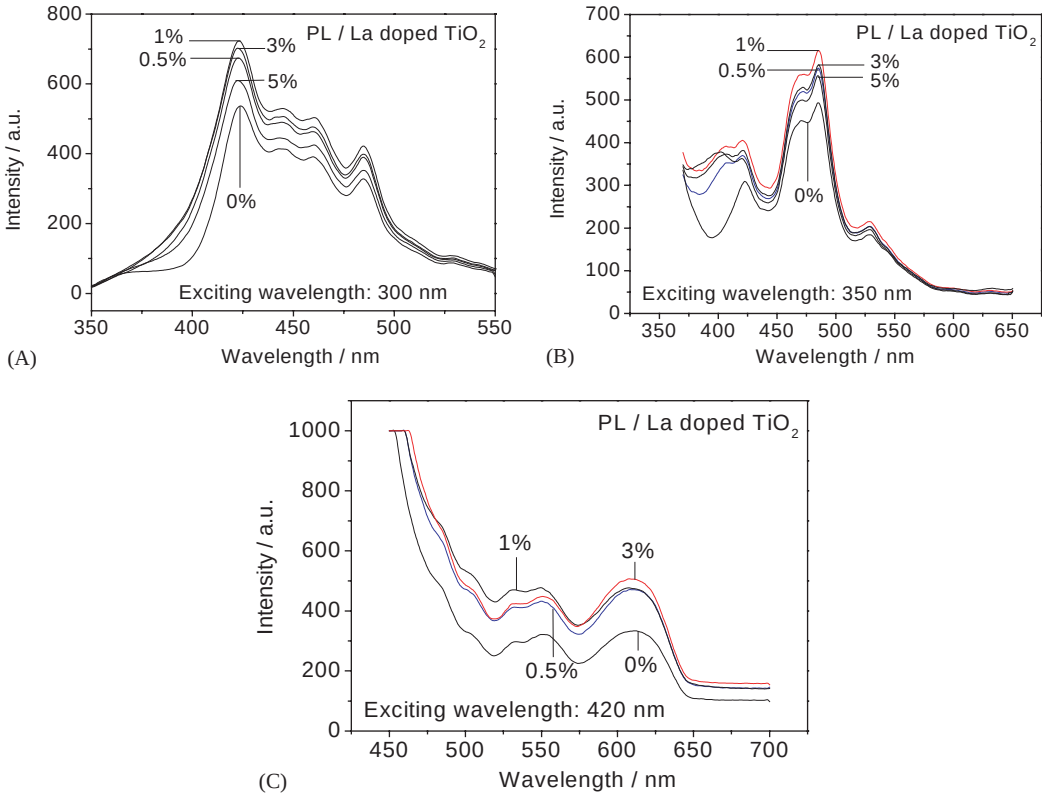

Fig. 6. (A–C) PL spectra of pure and La doped TiO_2 nanoparticles calcined at 600°C with different exciting wavelength.

vacancies very easily bind electrons to form excitons. Thus, the exciton energy level near the bottom of the conduction band could come into being, and the PL band of the excitons showed in Fig. 7 could also occur [19]. Our research group reported that there were lots of oxygen vacancies on the surface of ZnO nanoparticles, and proved that the oxygen vacancies had a strong ability to bind electrons by the means of EPR measurements [20]. In general, the smaller the particle size, the larger the oxygen vacancy content, the higher the probability of exciton occurrence, the stronger the PL signal [19].

In addition, it could be found from Fig. 6a that the threshold of PL response at the short wavelength edge of TiO_2 nanoparticles shifted to the blue after La was doped, and the PL intensity was also improved. This was because La dopant could inhibit the crystallite growth and the phase transformation of TiO_2 nanoparticles so that the surface content of oxygen vacancy or defect increased. The PL intensity gradually increased as La content increased, and arrived at the highest degree when La content was 1 mol%. If La content continued to increase, namely more than 1 mol%, the PL intensity began to go down. There were two possible reasons. One was that the effective area for absorbing light of TiO_2 nanoparticles decreased. Another was that lots of chemical bonds of Ti–O–La three element could occur so that the content of surface oxygen vacancy and defect

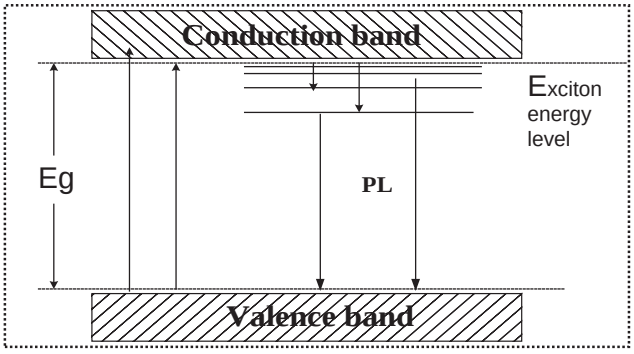

Fig. 7. Schematic diagram of exciton energy level between the conduction band and valence band and PL occurrence on the surface of semiconductor nanoparticles.

decreased [16]. Therefore, the PL intensity of TiO_2 nanoparticles could increase when appropriate content of La was doped, while it could decrease when too much content of La was doped.

It could be found from Fig. 6b that the range of PL response with excited wavelength of 350 nm expanded a little, and the PL spectra had obvious differences in curve shape as compared with that with excited wavelength of 300 nm, namely, new PL peak at about 525 nm occurred, although the used excited energies both were higher than the band gap energy. These demonstrated that PL mechanism of TiO_2 nanoparticles

was very complicated. Therefore, further research was needed.

Fig. 6c showed the PL spectrum with an excited wavelength of 420 nm, have two obvious PL peaks at about 550 and 615 nm, respectively. Since the used excited energy was lower than the band gap energy of TiO_2, the PL signal mainly resulted from the electron transitions related to surface defects or surface state energy level other than the electron transitions between the conduction band and valence band [8,17,18].

3.5. Measurement of photocatalytic activity

Fig. 8 showed the photocatalytic degradation curves of phenol on 5 mol% La doped TiO_2 nanoparticles calcined at different temperature, it could be found that the sample calcined at 600°C exhibited the highest photocatalytic activity, indicating that 600°C was the most appropriate calcination temperature.

Fig. 9 showed the photocatalytic degradation rate of phenol on La doped TiO_2 nanoparticles calcined at 600°C for 2 h with different content of La, reflecting the effects of La content on photocatalytic activity. According to Fig. 9, the order of photocatalytic activity of La doped TiO_2 nanoparticles was as following: $1>1.5>3>0.5>5>0$ mol%. Moreover, according to Fig. 6a, it should be pointed that the order of photocatalytic activity was the same as that of PL intensity, namely, the stronger the PL intensity, the higher the photocatalytic activity.

During the process of PL, oxygen vacancies and defects could bind photoinduced electrons to form free or binding excitons so that PL signal could easily occur, and the larger the content of oxygen vacancies or defects, the stronger the PL intensity. But, during the process of photocatalytic reactions, oxygen vacancies and defects could become the centers to capture photoinduced electrons so that the recombination of photoinduced electrons and holes could be effectively

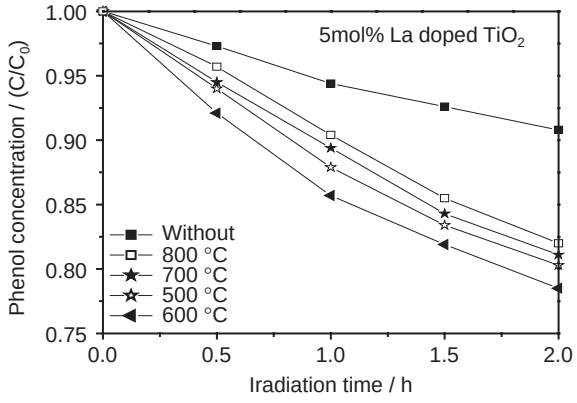

Fig. 8. The photocatalytic degradation curves of phenol on 5 mol% La doped TiO_2 nanoparticles calcined at different temperature.

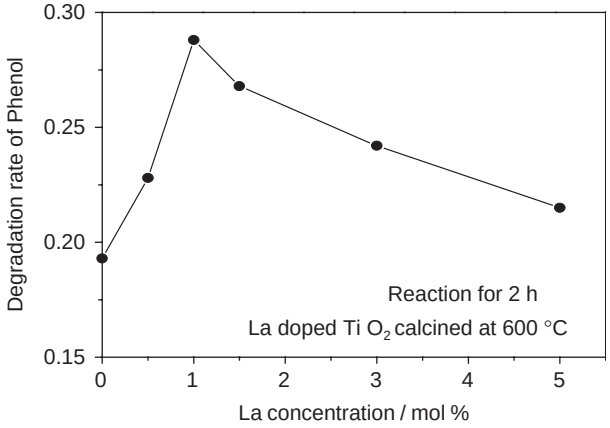

Fig. 9. The photocatalytic degradation rate of phenol on La doped TiO_2 nanoparticles calcined at 600°C for 2 h with different content of La.

inhibited. Moreover, oxygen vacancies could promote the adsorption of O_2, and there was strong interaction between the photoinduced electrons bound by oxygen vacancies and adsorbed O_2. This indicated that the binding for photoinduced electrons of oxygen vacancies could make for the capture for photoinduced electrons of adsorbed O_2, and $\cdot O_2$ free group was produced at the same time. Thus, oxygen vacancies and defects were in favor of photocatalytic reactions in that $\cdot O_2$ was active to promote the oxidation of organic substances [20,21].

The above results demonstrated that there were certain relationships between PL spectra and photocatalytic activity, namely, the stronger the PL intensity, the larger the content of oxygen vacancies and defects, the higher the photocatalytic activity. This could suggest that the photocatalytic activity of La doped TiO_2 samples be rapidly evaluated by the measurements of PL spectra at a certain degree.

4. Conclusions

We have prepared and characterized pure and La doped TiO_2 nanoparticles, and mainly investigated the relationships between PL spectra and photocatalytic activity as well as the effect mechanism of La on TiO_2 phase transformation. The results showed that La dopant had a great inhibition on TiO_2 phase transformation, and did not give rise to a new PL signal, but it could improve the intensity of PL spectra with a appropriate La content, attributed to the increase in the content of surface oxygen vacancies and defects. In addition, we found that the order of photocatalytic activity of La doped TiO_2 samples with different La content was the same as that of their PL intensity. This was because there were certain relationships between PL spectra and photocatalytic activity, namely, the stronger the PL intensity, the larger the content of oxygen

vacancies and defects, the higher the photocatalytic activity. Therefore, the photocatalytic activity of La doped TiO_2 samples could be rapidly evaluated by the measurement of PL spectra.

Acknowledgments

This work was supported by the National Nature Science Foundation of China (No.20171016, 20301006), the Nature Science Foundation of Heilongjiang Province of China (No. B0305), the Science Foundation for Excellent Youth of Heilongjiang Province of China (2002), the supporting plan of Education Bureau of Heilongjiang province (1054G035), and the Science Foundation for Excellent Youth of Heilongjiang University of China (2003).

References

[1] D.A. Tryk, A. Fujisshima, K. Honda, Electrochim. Acta 45 (15/16) (2000) 2363–2376.
[2] Y. Murata, S. Fukuta, S. Ishikawa, S. Yokoyama, Sol. Energy Mater. Sol. Cell 62 (1/2) (2000) 157–165.
[3] M.R. Hoffman, S.T. Martin, W. Choi, D.W. Bahnemann, Chem. Rev. 95 (1) (1995) 69–96.
[4] I. Litter Marta, Appl. Catal. B 23 (2/3) (1999) 89–114.
[5] A. Fujishima, T.N. Rao, D.A. Tryk, J. Photochem. Photobiol. C 1 (1) (2000) 1–21.
[6] K. Wilke, H.D. Breue, J. Photochem. Photobiol. A 121 (1999) 49–53.
[7] Liang Jinsheng, Jin Zongzhe, Wang Jing, et al., J. Chin. Ceram. Soc. 27 (5) (1999) 601–604.
[8] W.F. Zhang, M.S. Zhang, Z. Yin, Q. Chen, Appl. Phys. B 70 (2000) 261–265.
[9] H. Yamashita, Y. Ichihashi, S.G. Zhang, et al., Appl. Surf. Sci. 121/122 (1997) 305–311.
[10] X.Z. Li, F.B. Li, C.L. Yang, et al., J. Photochem. Photobiol. A 141 (2001) 209–217.
[11] L.Q. Jing, X.J. Sun, W.M. Cai, et al., J. Phys. Chem. Solid 64 (2003) 615–623.
[12] Q.H. Zhang, L. Gao, J.K. Guo, Appl. Catal. B 26 (2000) 207–215.
[13] Yin Lisong, Zhou Qifa, Tang Xingui, et al. Chin. Funct. Mater. 30 (5) (1999) 498–500.
[14] L.Q. Jing, Z.L. Xu, X.J. Sun, et al., Appl. Surf. Sci. 180 (2001) 308–314.
[15] R. Rodrguez-Talaveraa, S. Vargas, R. Aarroyo-Murillo, et al., J. Mater. Res. 12 (1997) 439–442.
[16] J. Lin, J.C. Yu, J. Photochem. Photobiol. A 116 (1998) 63–67.
[17] L.D. Zhang, C.M. Mo, Nanostruct. Mater. 6 (1995) 831–834.
[18] Li Danzhen, Zheng Yi, Fu Xianzhi, Chin. J. Mater. Res. 14 (6) (2000) 639–644.
[19] Zhang Lide, Mou Jimei, Nanomaterials and Nanostructure, Science Press, Beijing, 2001, p. 312.
[20] Jing Liqiang, Zheng Yingguang, Xu Zili, et al., Chem. J. Chin. Univ. 22 (11) (2001) 1885–1888.
[21] Jing Liqiang, Xu Zili, Du Yaoguo, et al., Chem. J. Chin. Univ. 23 (5) (2002) 871–875.